



ICCUB-11-165
NT@UW-11-21
NT-LBNL-11-017
UCB-NPAT-11-012
UNH-11-5

The Deuteron and Exotic Two-Body Bound States from Lattice QCD

S.R. Beane,¹ E. Chang,² W. Detmold,^{3,4} H.W. Lin,⁵ T.C. Luu,⁶
K. Orginos,^{3,4} A. Parreño,² M.J. Savage,⁵ A. Torok,⁷ and A. Walker-Loud⁸

(NPLQCD Collaboration)

¹*Department of Physics, University of New Hampshire, Durham, NH 03824-3568, USA*

²*Dept. d'Estructura i Constituents de la Matèria. Institut de Ciències del Cosmos (ICC),
Universitat de Barcelona, Martí i Franquès 1, E08028-Spain*

³*Department of Physics, College of William and Mary,
Williamsburg, VA 23187-8795, USA*

⁴*Jefferson Laboratory, 12000 Jefferson Avenue, Newport News, VA 23606, USA*

⁵*Department of Physics, University of Washington,
Box 351560, Seattle, WA 98195, USA*

⁶*N Division, Lawrence Livermore National Laboratory, Livermore, CA 94551, USA*

⁷*Department of Physics, Indiana University, Bloomington, IN 47405, USA*

⁸*Lawrence Berkeley National Laboratory, Berkeley, CA 94720, USA*

(Dated: November 6, 2018 - 14:30)

Abstract

Results of a high-statistics, multi-volume Lattice QCD exploration of the deuteron, the di-neutron, the H-dibaryon, and the $\Xi^- \Xi^-$ system at a pion mass of $m_\pi \sim 390$ MeV are presented. Calculations were performed with an anisotropic $n_f = 2 + 1$ Clover discretization in four lattice volumes of spatial extent $L \sim 2.0, 2.5, 3.0$ and 4.0 fm, with a lattice spacing of $b_s \sim 0.123$ fm in the spatial-direction, and $b_t \sim b_s/3.5$ in the time-direction. The $\Xi^- \Xi^-$ is found to be bound by $B_{\Xi^- \Xi^-} = 14.0(1.4)(6.7)$ MeV, consistent with expectations based upon phenomenological models and low-energy effective field theories constrained by nucleon-nucleon and hyperon-nucleon scattering data at the physical light-quark masses. We find weak evidence that both the deuteron and the di-neutron are bound at this pion mass, with binding energies of $B_d = 11(05)(12)$ MeV and $B_{nn} = 7.1(5.2)(7.3)$ MeV, respectively. With an increased number of measurements and a refined analysis, the binding energy of the H-dibaryon is $B_H = 13.2(1.8)(4.0)$ MeV at this pion mass, updating our previous result.

Contents

I. Introduction	3
II. Lattice QCD Calculations	4
A. Lüscher's Method for Two-Body Systems Including Bound States	4
B. Computational Overview	7
III. Baryons and Their Dispersion Relations	7
IV. Two-Body Bound States	9
A. The Deuteron	10
B. The Di-Neutron	13
C. The H-Dibaryon	15
D. $\Xi^- \Xi^-$	18
E. $\Sigma^- \Sigma^-$	20
V. Conclusions	21
References	23

I. INTRODUCTION

A major objective for nuclear physicists is to establish the technology with which to reliably calculate the properties and interactions of nuclei and to be able to quantify the uncertainties in such calculations. Achieving this objective will have broad impact, from establishing the behavior of matter under extreme conditions such as those that arise in the interior of neutron stars, to refining predictions for the array of isotopes produced in nuclear reactors, and even to answering anthropic questions about the nature of our universe. While nuclear phenomenology generally describes experimentally measured quantities, its ability to make high precision and accurate predictions for quantities that cannot be accessed experimentally is limited. This situation is on the verge of dramatically improving. The underlying theory of the strong interactions is known to be quantum chromodynamics (QCD), and the computational resources now available are beginning to allow for *ab initio* calculations of basic quantities in nuclear physics. With further increases in computational power and advances in algorithms, this trend will continue and our understanding of, and our ability to calculate, light and exotic nuclei will be placed on a solid foundation.

In nature, two nucleons in the ${}^3S_1 - {}^3D_1$ coupled channels bind to form the simplest nucleus, the deuteron ($J^\pi = 1^+$), with a binding energy of $B_d = 2.224644(34)$ MeV, and nearly bind into a di-neutron in the 1S_0 channel. However, little is known experimentally about possible bound states in more exotic channels, for instance those containing strange quarks. The most famous exotic channel that has been postulated to support a bound state (the H-dibaryon [1]) has the quantum numbers of $\Lambda\Lambda$ (total angular momentum $J^\pi = 0^+$, isospin $I = 0$ and strangeness $s = -2$). In this channel, all six quarks in naive quark models, like the MIT bag model, can be in the lowest-energy single-particle state. Additionally, more extensive analyses using one-boson-exchange (OBE) models [2] and low-energy effective field theories (EFT) [3, 4], both constrained by experimentally measured nucleon-nucleon (NN) and hyperon-nucleon (YN) cross-sections and the approximate SU(3) flavor symmetry of the strong interactions, suggest that other exotic channels also support bound states. In the limit of SU(3) flavor symmetry, the 1S_0 -channels are in symmetric irreducible representations of $\mathbf{8} \otimes \mathbf{8} = \mathbf{27} \oplus \mathbf{10} \oplus \overline{\mathbf{10}} \oplus \mathbf{8} \oplus \mathbf{8} \oplus \mathbf{1}$, and hence the $\Xi^-\Xi^-$, $\Sigma^-\Sigma^-$, and nn (along with $n\Sigma^-$ and $\Sigma^-\Xi^-$) all transform in the $\mathbf{27}$. YN and NN scattering data along with the leading SU(3) breaking effects, arising from the light-meson and baryon masses, suggest that $\Xi^-\Xi^-$ and $\Sigma^-\Sigma^-$ are bound at the physical values of the light-quark masses [2, 3, 4].

Recently, the first steps have been taken towards calculating the binding energies of light nuclei directly from QCD. Early exploratory quenched calculations of the NN scattering lengths [5, 6] performed more than a decade ago have been superseded by $n_f = 2 + 1$ calculations within the last few years [7, 8] (and added to by further quenched calculations [9, 10]¹). Further, the first quenched calculations of the deuteron [12], ${}^3\text{He}$ and ${}^4\text{He}$ [13] have been performed, along with $n_f = 2 + 1$ calculations of ${}^3\text{He}$ [14] and multi-baryon systems containing strange quarks [14]. Efforts to explore nuclei and nuclear matter using the strong coupling limit of QCD have led to some interesting observations [15]. Recently, $n_f = 2 + 1$ calculations by us (NPLQCD) [16], and subsequent $n_f = 3$ calculations by the HALQCD collaboration [17], have provided evidence that the H-dibaryon (with the quantum

¹ The HALQCD collaboration has produced non-local, energy-dependent, and sink-operator dependent quantities from lattice spatial correlation functions that contain the same, but no more, information than the NN energy eigenvalues in the lattice volume(s), e.g. Ref. [11].

numbers of $\Lambda\Lambda$) is bound at a pion mass of $m_\pi \sim 390$ MeV [NPLQCD] and $m_\pi \sim 837$ MeV [HALQCD]². Extrapolations to the physical light-quark masses suggest a weakly bound H-dibaryon or a near threshold resonance exists in this channel [18, 19].

In this work, which is a continuation of our high-statistics Lattice QCD explorations [8, 14, 20, 21], we present evidence for $\Xi^-\Xi^-(^1S_0)$ and H-dibaryon (refining of our results presented in Ref. [16]) bound states, and weak evidence for a bound deuteron and di-neutron at a pion mass of $m_\pi \sim 390$ MeV. The results were obtained from four ensembles of $n_f = 2 + 1$ anisotropic clover gauge-field configurations with a spatial lattice spacing of $b_s \sim 0.123$ fm, an anisotropy of $\xi \sim 3.5$ and with cubic volumes of spatial extent $L \sim 2.0, 2.5, 3.0$ and 4.0 fm.

In section II, a concise description of the specific LQCD technology and computational details relevant to the present two-body bound state calculations are given. Section III presents the results of the LQCD calculations of the single baryon masses and dispersion relations (critical for understanding bound systems), and in section IV the results for the bound states are presented. Discussions and our conclusions can be found in section V.

II. LATTICE QCD CALCULATIONS

Lattice QCD (LQCD) is a technique in which space-time is discretized into a four-dimensional grid and the QCD path integral over the quark and gluon fields at each point in the grid is performed in Euclidean space-time using Monte Carlo methods. A LQCD calculation of a given quantity will differ from its actual value because of the finite volume of the space-time (with $L^3 \times T$ lattice points) over which the fields exist, and the finite separation between space-time points (the lattice-spacing). However, such deviations can be systematically removed by performing calculations in multiple volumes with multiple lattice spacings, and extrapolating using the theoretically known functional dependences on each. In the following subsections, we review the details of LQCD calculations relevant to the current work and introduce the ensembles studied herein.

A. Lüscher's Method for Two-Body Systems Including Bound States

The hadron-hadron scattering amplitude below the inelastic threshold can be determined from two-hadron energy levels in the lattice volume using Lüscher's method [22, 23, 24]. In the situation where only a single scattering channel is kinematically allowed, the deviation of the energy eigenvalues of the two-hadron system in the lattice volume from the sum of the single-hadron energies is related to the scattering phase shift, $\delta(k)$, at the measured two-hadron energies. For energy eigenvalues above kinematic thresholds where multiple channels contribute, a coupled-channels analysis is required as a single phase shift does not parameterize the S-matrix. Such analyses can be performed, but they are not required in the current context. The energy shift for two particles A and B , $\Delta E = E_{AB} - E_A - E_B$, can be determined from the correlation functions for systems containing one and two hadrons.

² One should note that both calculations were performed at approximately the same spatial lattice spacing of $b \sim 0.12$ fm.

For baryon-baryon systems, correlation functions of the form

$$C_{\mathcal{B};\Gamma}(\mathbf{p}, t) = \sum_{\mathbf{x}} e^{i\mathbf{p}\cdot\mathbf{x}} \Gamma_{\alpha}^{\beta} \langle \mathcal{B}_{\alpha}(\mathbf{x}, t) \bar{\mathcal{B}}_{\beta}(\mathbf{x}_0, 0) \rangle \quad (1)$$

$$C_{\mathcal{B}_1, \mathcal{B}_2; \Gamma}(\mathbf{p}_1, \mathbf{p}_2, t) = \sum_{\mathbf{x}_1, \mathbf{x}_2} e^{i\mathbf{p}_1 \cdot \mathbf{x}_1} e^{i\mathbf{p}_2 \cdot \mathbf{x}_2} \Gamma_{\beta_1 \beta_2}^{\alpha_1 \alpha_2} \langle \mathcal{B}_{1, \alpha_1}(\mathbf{x}_1, t) \mathcal{B}_{2, \alpha_2}(\mathbf{x}_2, t) \bar{\mathcal{B}}_{1, \beta_1}(\mathbf{x}_0, 0) \bar{\mathcal{B}}_{2, \beta_2}(\mathbf{x}_0, 0) \rangle ,$$

are used, where \mathcal{B} denotes a baryon interpolating operator, α_i and β_i are Dirac indices, and the Γ are Dirac matrices that typically project onto particular parity and angular momentum states. The $\langle \dots \rangle$ denote averaging over the gauge-field configurations and \mathbf{x}_0 is the location of the source. The interpolating operators are only constrained by the quantum numbers of the system of interest, and the simplest forms are

$$\begin{aligned} p_{\alpha}(\mathbf{x}, t) &= \epsilon^{ijk} u_{\alpha}^i(\mathbf{x}, t) \left[u^{j\Gamma}(\mathbf{x}, t) C \gamma_5 d^k(\mathbf{x}, t) \right] , \\ \Lambda_{\alpha}(\mathbf{x}, t) &= \epsilon^{ijk} s_{\alpha}^i(\mathbf{x}, t) \left[u^{j\Gamma}(\mathbf{x}, t) C \gamma_5 d^k(\mathbf{x}, t) \right] , \\ \Sigma_{\alpha}^{+}(\mathbf{x}, t) &= \epsilon^{ijk} u_{\alpha}^i(\mathbf{x}, t) \left[u^{j\Gamma}(\mathbf{x}, t) C \gamma_5 s^k(\mathbf{x}, t) \right] , \\ \Xi_{\alpha}^0(\mathbf{x}, t) &= \epsilon^{ijk} s_{\alpha}^i(\mathbf{x}, t) \left[u^{j\Gamma}(\mathbf{x}, t) C \gamma_5 s^k(\mathbf{x}, t) \right] , \end{aligned} \quad (2)$$

where C is the charge-conjugation matrix and ijk are color indices. Other hadrons in the lowest-lying octet can be obtained from the appropriate combinations of quark flavors. The brackets in the interpolating operators indicate contraction of spin indices into a spin-0 “diquark”. Away from the time slice of the source (in this case $t = 0$), these correlation functions behave as

$$C_{\mathcal{H}_A}^{(i,f)}(\mathbf{p}, t) = \sum_n Z_{n;A}^{(i)}(\mathbf{p}) Z_{n;A}^{(f)}(\mathbf{p}) e^{-E_n^{(A)}(\mathbf{p}) t} , \quad (3)$$

$$C_{\mathcal{H}_A \mathcal{H}_B}^{(i,f)}(\mathbf{p}, -\mathbf{p}, t) = \sum_n Z_{n;AB}^{(i)}(\mathbf{p}) Z_{n;AB}^{(f)}(\mathbf{p}) e^{-E_n^{(AB)}(\mathbf{0}) t} , \quad (4)$$

where $E_0^{(A)}(\mathbf{0}) = m_A$ and $E_n^{(AB)}(\mathbf{0})$ are the energy eigenvalues of the two-hadron system at rest in the lattice volume. The quantities $Z_{n;X}^{(i)}$ ($Z_{n;X}^{(f)}$) are determined by the overlap of the source (sink) onto the n^{th} energy eigenstate with the quantum numbers of X . At large times, the ratio

$$\frac{C_{\mathcal{H}_A \mathcal{H}_B}^{(i,f)}(\mathbf{p}, -\mathbf{p}, t)}{C_{\mathcal{H}_A}^{(i,f)}(\mathbf{0}, t) C_{\mathcal{H}_B}^{(i,f)}(\mathbf{0}, t)} \xrightarrow{t \rightarrow \infty} \tilde{Z}_{0,AB}^{(i)}(\mathbf{p}) \tilde{Z}_{0,AB}^{(f)}(\mathbf{p}) e^{-\Delta E_0^{(AB)}(\mathbf{0}) t} \quad (5)$$

decays as a single exponential in time with the energy shift, $\Delta E_0^{(AB)}(\mathbf{0})$. In what follows, only the case $\mathbf{p} = \mathbf{0}$ is considered. The energy shift of the n^{th} two-hadron state,

$$\Delta E_n^{(AB)} \equiv E_n^{(AB)}(\mathbf{0}) - m_A - m_B = \sqrt{k_n^2 + m_A^2} + \sqrt{k_n^2 + m_B^2} - m_A - m_B , \quad (6)$$

determines a squared momentum, k_n^2 (which can be either positive or negative). Below inelastic thresholds, this is related to the real part of the inverse scattering amplitude via ³

$$k_n \cot \delta(k_n) = \frac{1}{\pi L} S \left(k_n^2 \left(\frac{L}{2\pi} \right)^2 \right), \quad (7)$$

where

$$S(x) = \lim_{\Lambda \rightarrow \infty} \sum_{|\mathbf{j}| < \Lambda} \frac{1}{|\mathbf{j}|^2 - x} - 4\pi \Lambda, \quad (8)$$

thereby implicitly determining the value of the phase shift at the energy $\Delta E_n^{(AB)}$ (or the momentum of each particle in the center of momentum (CoM) frame, k_n), $\delta(k_n)$ [22, 23, 24, 25, 26]. Thus, the function $k \cot \delta$ that determines the low-energy elastic-scattering cross-section, $\mathcal{A}(k) \propto (k \cot \delta(k) - ik)^{-1}$, is determined at the energy $\Delta E_n^{(AB)}$.

In a channel for which one pion exchange (OPE) is allowed by spin and isospin considerations, the function $k \cot \delta(k)$ is an analytic function of $|\mathbf{k}|^2$ for $|\mathbf{k}| \leq m_\pi/2$, as determined by the t -channel cut in the scattering amplitude. In this kinematic regime, $k \cot \delta(k)$ can be expressed in terms of an effective range expansion (ERE) of the form

$$k \cot \delta(k) = -\frac{1}{a} + \frac{1}{2} r_0 |\mathbf{k}|^2 + \dots, \quad (9)$$

where a is the scattering length (with the nuclear physics sign convention) and r_0 is the effective range. While the magnitude of the effective range (and higher terms) is set by the pion mass, the scattering length is unconstrained. For scattering processes where OPE does not contribute, the radius of convergence of the ERE of $k \cot \delta$ is set by the lightest intermediate state in the t -channel (or by the inelastic threshold).

In the situation where a channel supports a bound state, the energy of the bound state at rest is determined by eq. (7). For $k_{-1}^2 < 0$, and setting $k_{-1} = i\kappa$, eq. (7) becomes

$$k \cot \delta(k)|_{k=i\kappa} + \kappa = \frac{1}{L} \sum_{\mathbf{m} \neq \mathbf{0}} \frac{1}{|\mathbf{m}|} e^{-|\mathbf{m}|\kappa L} = \frac{1}{L} F^{(0)}(\kappa L), \quad (10)$$

where

$$F^{(0)}(\kappa L) = 6 e^{-\kappa L} + 6\sqrt{2} e^{-\sqrt{2}\kappa L} + \frac{8}{\sqrt{3}} e^{-\sqrt{3}\kappa L} + \dots \quad (11)$$

Perturbation theory can be used to solve eq. (10) when the extent of the volume is much larger than the size of the bound system, giving [25, 26]

$$\kappa = \kappa_0 + \frac{Z_\psi^2}{L} F^{(0)}(\kappa_0 L) + \mathcal{O}(e^{-2\kappa_0 L}/L) \quad \text{with} \quad Z_\psi = \frac{1}{\sqrt{1 - 2\kappa_0 \frac{d}{dk^2} k \cot \delta|_{i\kappa_0}}}. \quad (12)$$

³ Calculations performed on anisotropic lattices require a modified energy-momentum relation, and, as a result, eq. (6) becomes

$$\Delta E_n^{(AB)} \equiv E_n^{(AB)} - m_A - m_B = \sqrt{k_n^2/\xi_A^2 + m_A^2} + \sqrt{k_n^2/\xi_B^2 + m_B^2} - m_A - m_B,$$

where $\xi_{A,B}$ are the anisotropy factors for particle A and particle B , respectively, determined from the appropriate energy-momentum dispersion relation. The masses and energy splitting are given in terms of temporal lattice units and k_n is given in spatial lattice units.

κ_0 is the solution to

$$k \cot \delta(k)|_{k=i\kappa_0} + \kappa_0 = 0 \quad , \quad (13)$$

which recovers $\cot \delta(k)|_{k=i\kappa_0} = +i$, and is the infinite-volume binding momentum of the system. This analysis has recently been extended to bound systems that are moving in the lattice volume [27, 28].

B. Computational Overview

Anisotropic gauge field configurations have proven useful for the study of hadronic spectroscopy, and as the calculations required for studying multi-hadron systems rely heavily on spectroscopy, considerable effort has been put into calculations with clover-improved Wilson fermion actions with an anisotropic discretization. In particular, the $n_f = 2 + 1$ flavor anisotropic Clover Wilson action [29, 30] with two steps of stout-link smearing [31] of the spatial gauge fields in the fermion action with a smearing weight of $\rho = 0.14$ has been used [32, 33]. The gauge fields entering the fermion action are not smeared in the time direction, thus preserving the ultra-locality of the action in the time direction. Further, a tree-level tadpole-improved Symanzik gauge action without a 1×2 rectangle in the time direction is used. Anisotropy allows for a better extraction of the excited states as well as additional confidence that plateaus in the effective mass plots (EMPs) formed from the correlation functions have been observed, significantly reducing the systematic uncertainties. The gauge field generation was performed by the Hadron Spectrum Collaboration (HSC) and by us, and these gauge field configurations have been extensively used for excited hadron spectrum calculations by HSC [34, 35, 36, 37, 38, 39].

The present calculations are performed on four ensembles of gauge configurations with $L^3 \times T$ of $16^3 \times 128$, $20^3 \times 128$, $24^3 \times 128$ and $32^3 \times 256$ lattice sites, with an anisotropy of $b_t = b_s/\xi$ with $\xi \sim 3.5$. The spatial lattice spacing of each ensemble is $b_s \sim 0.1227 \pm 0.008$ fm, giving spatial lattice extents of $L \sim 2.0, 2.5, 3.0$ and 4.0 fm respectively. The same input light-quark mass parameters, $b_t m_l = -0.0840$ and $b_t m_s = -0.0743$, are used in the production of each ensemble, giving a pion mass of $m_\pi \sim 390$ MeV. The relevant quantities to assign to each ensemble that determine the impact of the finite lattice volume are $m_\pi L$ and $m_\pi T$, which for the four ensembles are $m_\pi L \sim 3.86, 4.82, 5.79$ and 7.71 respectively, and $m_\pi T \sim 8.82, 8.82, 8.82$ and 17.64 .

For the four lattice ensembles, multiple light-quark propagators were calculated on each configuration. The source location was chosen randomly in order to minimize correlations among propagators. On the $\{16^3 \times 128, 20^3 \times 128, 24^3 \times 128, 32^3 \times 256\}$ ensembles, an average of $\{224, 364, 178, 174\}$ propagators were calculated on each of $\{2001, 1195, 2215, 739\}$ gauge field configurations, to give a total number of $\sim \{4.5, 4.3, 3.9, 1.3\} \times 10^5$ light-quark propagators, respectively.

III. BARYONS AND THEIR DISPERSION RELATIONS

The single hadron masses calculated in the four different lattice volumes are given in Table I. Detailed discussions of the fitting methods used in the analysis of the correlation functions are given in Ref. [8, 14, 20, 40]. Infinite volume extrapolations of the results obtained from the four ensembles were performed in Ref. [21], and are

TABLE I: Results from the Lattice QCD calculations in four lattice volumes with a pion mass of $m_\pi \sim 390$ MeV, a spatial lattice spacing of $b_s \sim 0.123$ fm, and with an anisotropy factor of $\xi \sim 3.5$. Infinite-volume extrapolations [21] are shown in the right column. The masses are in temporal lattice units (t.l.u.).

$L^3 \times T$	$16^3 \times 128$	$20^3 \times 128$	$24^3 \times 128$	$32^3 \times 256$	Extrapolation
L (fm)	~ 2.0	~ 2.5	~ 3.0	~ 4.0	∞
$m_\pi L$	3.86	4.82	5.79	7.71	∞
$m_\pi T$	8.82	8.82	8.82	17.64	∞
M_N (t.l.u.)	0.21004(44)(85)	0.20682(34)(45)	0.20463(27)(36)	0.20457(25)(38)	0.20455(19)(17)
M_Λ (t.l.u.)	0.22446(45)(78)	0.22246(27)(38)	0.22074(20)(42)	0.22054(23)(31)	0.22064(15)(19)
M_Σ (t.l.u.)	0.22861(38)(67)	0.22752(32)(43)	0.22791(24)(31)	0.22726(24)(43)	0.22747(17)(19)
M_Ξ (t.l.u.)	0.24192(38)(63)	0.24101(27)(38)	0.23975(20)(32)	0.23974(17)(31)	0.23978(12)(18)

shown in the right-most column in Table I. In physical units, the extrapolated baryon masses are $M_N = 1151.3(1.1)(1.0)(7.5)$ MeV, $M_\Lambda = 1241.9(0.8)(1.1)(8.1)$ MeV, $M_\Sigma = 1280.3(1.0)(1.1)(8.3)$ MeV, and $M_\Xi = 1349.6(0.7)(1.0)(8.8)$ MeV [21]. The difference between a mass calculated in a finite lattice volume and its infinite-volume extrapolation is due to contributions of the form $\sim e^{-m_\pi L}$. Such deviations must be small compared to the two-body binding energies to ensure that the finite volume bindings are due to the T-matrix [41, 42] and not from finite volume distortions of the forces. It has been shown [16, 21] that the largest two volumes, the $24^3 \times 128$ and $32^3 \times 256$ ensembles, are sufficiently large to render the $\sim e^{-m_\pi L}$ modifications to Lüscher's eigenvalue relation negligible at the level of precision we are currently able to achieve. In what follows, we only consider results from these ensembles.

Lüscher's method assumes that the single-hadron energy-momentum relation is satisfied over the range of energies used in eq. (7). In order to verify that the energy-momentum relation is satisfied, single hadron correlation functions were formed with well-defined lattice spatial momentum $\mathbf{p} = \frac{2\pi}{L}\mathbf{n}$ for $|\mathbf{n}|^2 \leq 5$. Retaining the leading terms in the energy-momentum relation, including the lattice anisotropy ξ , the energy and mass of the hadron (in temporal lattice units (t.l.u)), and the momentum in spatial lattice units (s.l.u) are related by

$$\left(b_t E_H(|\mathbf{n}|^2)\right)^2 = (b_t M_H)^2 + \frac{1}{\xi^2} \left(\frac{2\pi b_s}{L}\right)^2 |\mathbf{n}|^2. \quad (14)$$

The calculated single hadron energies (squared) are shown in fig. 1 as a function of $|\mathbf{n}|^2$, along with the best linear fit. The extracted values of ξ_H are given in Table II, and are seen to be consistent with each other within the uncertainties of the calculation (the value for the nucleon is somewhat larger). These values are used to convert the two-hadron energies and energy differences from temporal lattice units into spatial lattice units which are then used in the Lüscher eigenvalue relation.

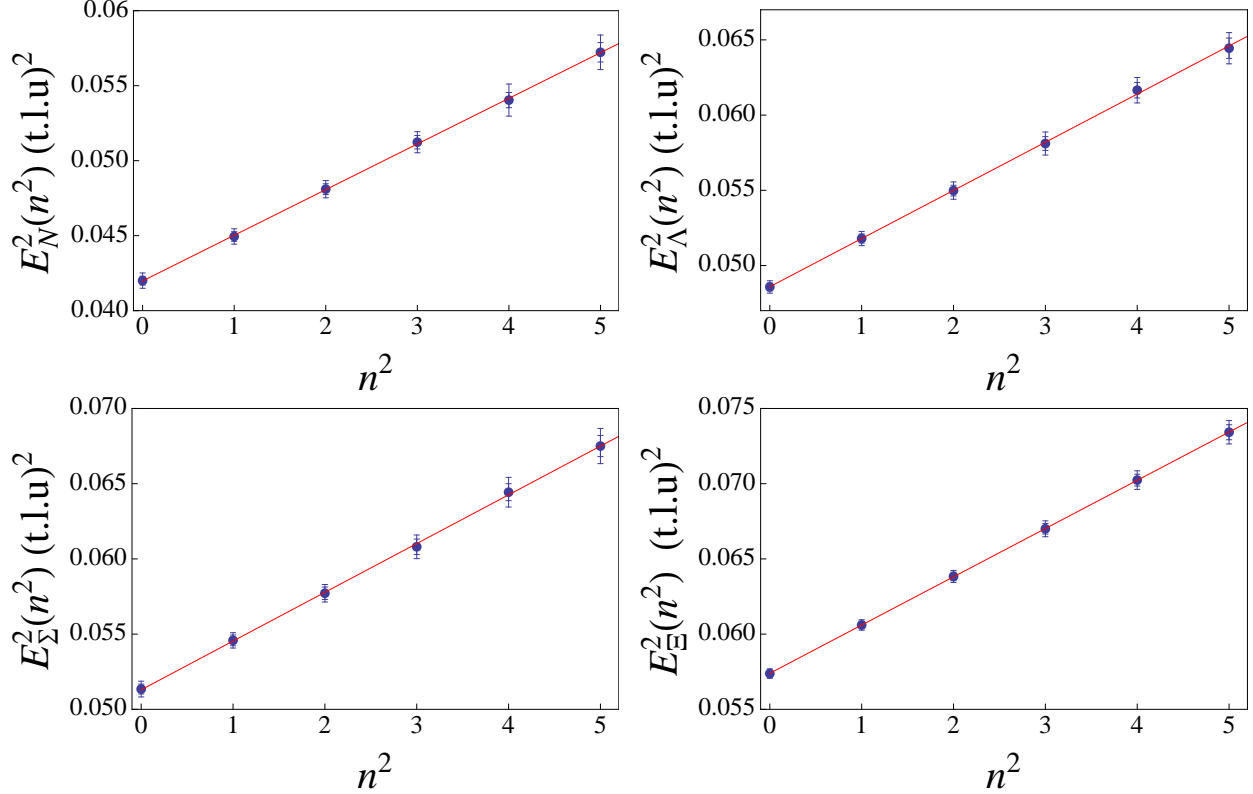


FIG. 1: The squared energy (in (t.l.u.)²) of the single baryon states as a function of $n^2 = |\mathbf{n}|^2$, related to the squared-momentum, $|\mathbf{p}|^2 = \left(\frac{2\pi}{L}\right)^2 |\mathbf{n}|^2$, calculated with the $32^3 \times 256$ ensemble. The blue points are the results of the LQCD calculations with the inner (outer) uncertainties being the statistical uncertainties (statistical and systematic uncertainties combined in quadrature). The red curves correspond to the best linear-fits.

TABLE II: The anisotropy parameter, ξ_H , of each hadron from the $32^3 \times 256$ ensemble. The result for the π is included for purposes of comparison.

	N	Λ	Σ	Ξ	π
ξ_H	3.559(27)(08)	3.465(31)(06)	3.456(35)(07)	3.4654(55)(14)	3.466(13)(02)

IV. TWO-BODY BOUND STATES

Of the baryon-baryon channels that we have explored at this pion mass, the states that have an energy lower than two isolated baryons in both the $24^3 \times 128$ and $32^3 \times 256$ ensembles and suggest the existence of bound states are the deuteron, the di-neutron, the H-dibaryon, and the $\Xi^- \Xi^-$. While a negative energy shift can indicate either a scattering state with an attractive interaction or a bound state, Lüscher's eigenvalue relation allows us to distinguish between the two possibilities. For a bound system in the large-volume limit, the calculated value of the energy splitting (or binding momentum) gives rise to $-i \cot \delta \rightarrow +1$. We now examine each of these channels.

A. The Deuteron

The deuteron is the simplest nucleus, comprised of a neutron and a proton. At the physical light-quark masses its binding energy is $B = 2.224644(34)$ MeV which corresponds to a binding momentum of $\kappa_0 \sim 45.70$ MeV (using the isospin averaged nucleon mass of $M_N = 938.92$ MeV). As it is a spin-1 system composed of two spin- $\frac{1}{2}$ nucleons, its wavefunction is an admixture of s-wave and d-wave, but at the physical quark masses it is known to be predominantly s-wave with only a small admixture of d-wave induced by the tensor ($L = S = 2$) interaction.

The EMPs associated with the nucleon and the neutron-proton system in the ${}^3S_1 - {}^3D_1$ channel are shown in the left panels of fig. 2 and fig. 3 for the two ensembles. The correlation functions that give rise to these EMPs are linear combinations of correlation functions generated using eq. (1) but with different smearings of the sink operator(s). The combinations of correlation functions have been chosen to maximize the extent of the ground-state plateaus⁴. Extended plateaus are observed in both the one and two nucleon correlation

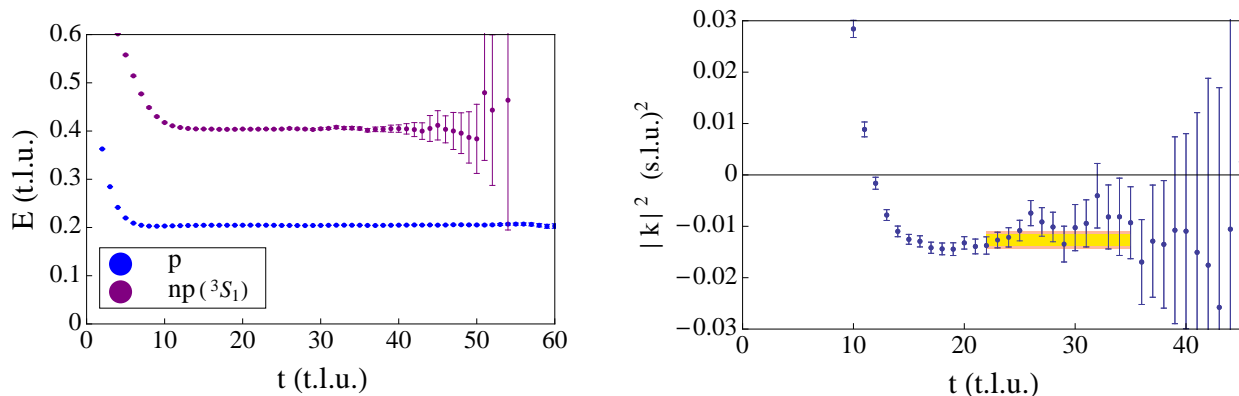


FIG. 2: The left panel shows an EMP of the nucleon and of the neutron-proton system in the ${}^3S_1 - {}^3D_1$ coupled channels calculated with the $24^3 \times 128$ ensemble (in t.l.u.). The right panel shows the $|k|^2$ (in (s.l.u.)²) of the neutron-proton system calculated with this ensemble, along with the fits.

functions. The right panels of fig. 2 and fig. 3 show the binding momentum of each particle in the CoM obtained by taking ratios of the two-baryon and single-baryon correlation functions. The deuteron binding energies in each volume calculated with LQCD are

$$B_d^{(L=24)} = 22.3 \pm 2.3 \pm 5.4 \text{ MeV} \quad , \quad B_d^{(L=32)} = 14.9 \pm 2.3 \pm 5.8 \text{ MeV} \quad . \quad (15)$$

The known finite-volume dependence of loosely bound systems, given in eq. (10), and the perturbative relations that follow, allow for an extrapolation of the results in eq. (15) to the infinite-volume limit, as shown in fig. 4, giving

$$B_d^{(L=\infty)} = 11 \pm 5 \pm 12 \text{ MeV} \quad (16)$$

⁴ The EMPs result from a matrix-Prony analysis [20] of multiple correlation functions. In determining the binding energies, multi-exponential fitting and generalized pencil of function (GPoF) methods [43, 44] are used in addition to Matrix-Prony and provides consistent results in each case.

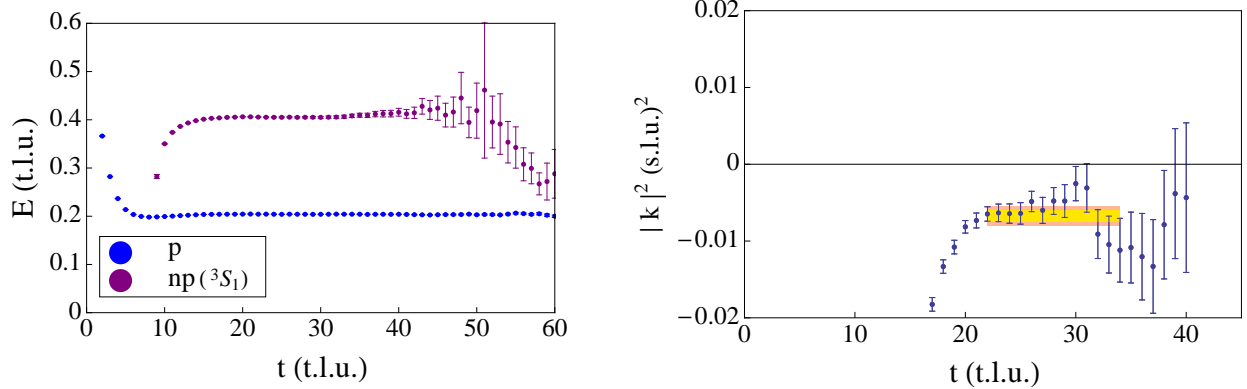


FIG. 3: The left panel shows an EMP of the nucleon and of the neutron-proton system in the ${}^3S_1 - {}^3D_1$ coupled channels calculated with the $32^3 \times 256$ ensemble (in t.l.u.). The right panel shows the $|\mathbf{k}|^2$ (in (s.l.u.) 2) of the neutron-proton system calculated with this ensemble, along with the fits.

where the first uncertainty is statistical and the second is systematic, accounting for fitting, anisotropy, lattice spacing and the infinite volume extrapolation. Despite having statistically

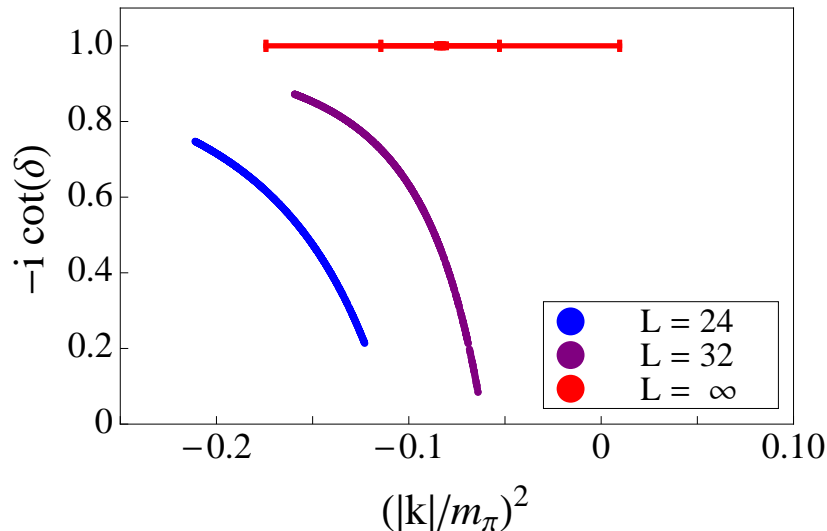


FIG. 4: Results of the Lattice QCD calculations of $-i \cot \delta$ versus $|\mathbf{k}|^2/m_\pi^2$ in the deuteron channel obtained using eq. (7), along with the infinite-volume extrapolation using eq. (10). The inner uncertainty of the infinite-volume extrapolation is statistical, while the outer corresponds to the statistical and systematic uncertainties combined in quadrature.

significant binding energies in the two lattice volumes, the exponential extrapolation to the infinite volume limit produces a deuteron binding energy with significance at $\sim 1\sigma$. If the uncertainties of both LQCD calculations were reduced by a factor of two, the significance of the extrapolated binding energy would increase to $\sim 3\sigma$ if the central values remained unchanged. From the curvature of the results of the LQCD calculations in fig. 4, it is clear the both of these volumes significantly modify the deuteron at this pion mass. Calcula-

tions in somewhat larger volumes, or of moving systems [28], would significantly reduce the uncertainty introduced by the volume extrapolation.

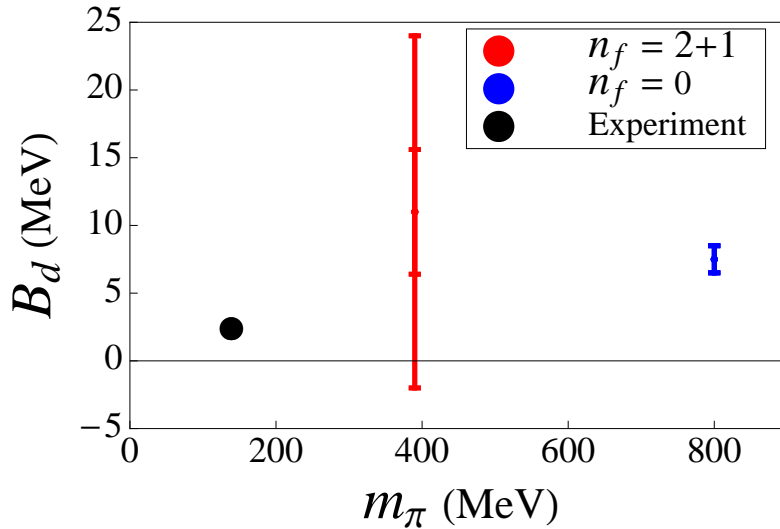


FIG. 5: The deuteron binding energy as a function of the pion mass. The black circle denotes the experimental value. The blue point and uncertainty results from the quenched calculations of Ref. [12], while the red point and uncertainty (the inner is statistical and the outer is statistical and systematic combined in quadrature) is our present $n_f = 2 + 1$ result.

Our $n_f = 2 + 1$ result and the recent quenched ($n_f = 0$) result of Ref. [12] are shown in fig. 5, along with the physical deuteron binding energy. Clearly, the large uncertainty of our present result does not provide much constraint on the dependence of the deuteron binding energy as a function of the light-quark masses, other than to demonstrate that the deuteron is likely bound at $m_\pi \sim 390$ MeV, qualitatively consistent with the quenched result at $m_\pi \sim 800$ MeV [12].

A number of groups have attempted to determine how the deuteron binding energy (and the binding of other nuclei) varies as a function of the light-quark masses using EFT [45, 46, 47, 48] and hadronic models [49]. Such a variation impacts the constraints that can be placed on possible time-variations of the fundamental constants of nature from the abundance of elements produced in Big Bang Nucleosynthesis (BBN) (see Refs. [50, 51] for recent constraints from BBN). With the exception of the analysis of Ref. [48], both of the EFT analyses, which use naive dimensional analysis (NDA) to constrain the quark-mass dependent dimension-six operators that contribute at next-to-leading order (NLO) in the chiral expansion, and the hadronic models of Ref. [49], suggest that the deuteron becomes less bound as the quarks become heavier near their physical values. The present LQCD calculation at a pion mass of $m_\pi \sim 390$ MeV is somewhat beyond the range of applicability of the EFT analyses and so cannot be directly translated into constraints on the coefficients of local operators with confidence. Further, the uncertainty in our calculation is too large to be useful in a quantitative way. Nevertheless, our result conflicts with the trend suggested in most of the EFT and model analyses, and further studies are necessary to resolve this issue.

B. The Di-Neutron

In nature, the di-neutron ($nn\ ^1S_0$) is very nearly bound. The unnaturally large scattering lengths in the 1S_0 -channel indicate that a very small increase in the strength of the interactions between neutrons would bind them into an electrically neutral nucleus. If the binding was deep enough, it would have profound effects on nucleosynthesis. Analyses with NNEFT allow for the possibility of both bound and unbound di-neutrons for light-quark masses larger than those of nature, while indicating an unbound di-neutron for lighter quark masses [45, 46, 47]. In contrast, a model-dependent calculation indicates that the di-neutron remains unbound for all light-quark masses [49].

The EMPs associated with the nucleon and the di-neutron system are shown in the left panels of fig. 6 and fig. 7. The di-neutron binding energies extracted from the LQCD

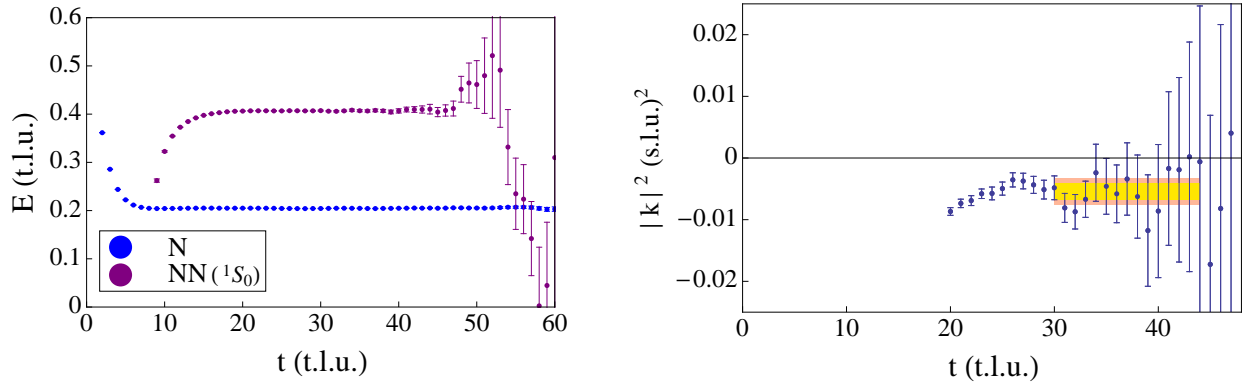


FIG. 6: The left panel shows an EMP of the neutron and of the neutron-neutron system calculated with the $24^3 \times 128$ ensemble (in t.l.u.). The right panel shows the $|k|^2$ (in (s.l.u.) 2) of the neutron-neutron system calculated with this ensemble, along with the fits.

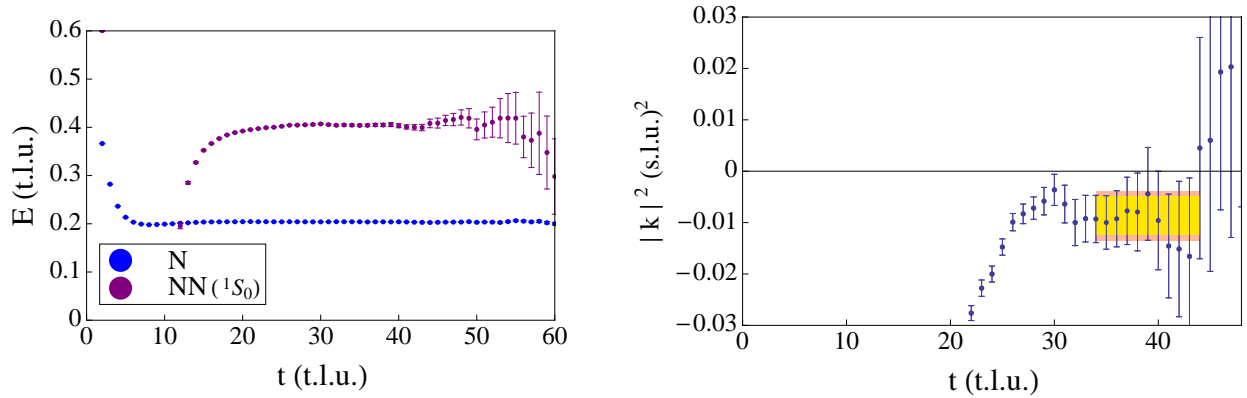


FIG. 7: The left panel shows an EMP of the neutron and of the neutron-neutron system calculated with the $32^3 \times 256$ ensemble (in t.l.u.). The right panel shows the $|k|^2$ (in (s.l.u.) 2) of the neutron-neutron system calculated with this ensemble, along with the fits.

calculations are

$$B_{nn}^{(L=24)} = 10.4 \pm 2.6 \pm 3.1 \text{ MeV} \quad , \quad B_{nn}^{(L=32)} = 8.3 \pm 2.2 \pm 3.3 \text{ MeV} \quad . \quad (17)$$

The volume extrapolation of the results in eq. (17) is shown in fig. 8, and results in an extrapolated di-neutron binding energy of

$$B_{nn}^{(L=\infty)} = 7.1 \pm 5.2 \pm 7.3 \text{ MeV} \quad (18)$$

where the first uncertainty is statistical and the second is systematic. This result is suggestive

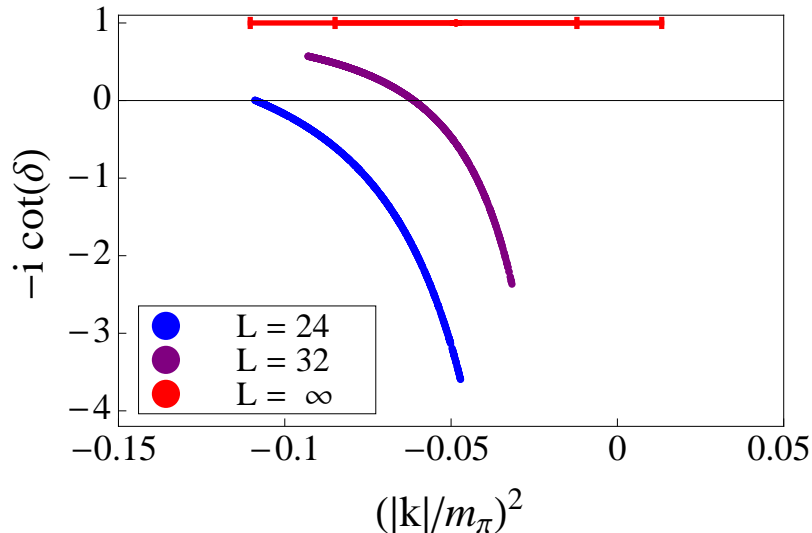


FIG. 8: The results of the Lattice QCD calculations of $-i \cot \delta$ versus $|\mathbf{k}|^2/m_\pi^2$ in the di-neutron channel obtained using eq. (7), along with the infinite-volume extrapolation using eq. (10). The inner uncertainty of the infinite-volume extrapolation is statistical, while the outer corresponds to the statistical and systematic uncertainties combined in quadrature.

of a bound di-neutron at this pion mass, but at the present level of precision an unbound system is also possible.

Our $n_f = 2 + 1$ result and the recent quenched ($n_f = 0$) result of Ref. [12] are shown in fig. 9. Clearly, the large uncertainty of our present result does not provide a significant constraint on the binding of the di-neutron as a function of the light-quark masses. However, the LQCD results suggest that the di-neutron is bound at quark masses greater than those of nature. This has implication for future LQCD calculations as there are likely light-quark masses for which the di-neutron unbinds, and hence the scattering length becomes infinitely large. This implies that, at some point in the future, LQCD may be able to explore strongly interacting systems of fermions near the unitary limit. However, if the deuteron remains bound at heavier quark masses, as suggested by the current work, it may not be possible to tune the light-quark masses (including isospin breaking) to produce infinite scattering lengths in the ${}^3S_1 - {}^3D_1$ and 1S_0 channels simultaneously and hence eliminating the possibility of the triton having an infinite number of bound states for such a specific choice of light-quark masses (unless the deuteron is also unbound for an intermediate range of quark masses)⁵.

⁵ Such bound states would be the manifestation of an infrared renormalization group limit cycle in QCD, as conjectured by Braaten and Hammer [52].

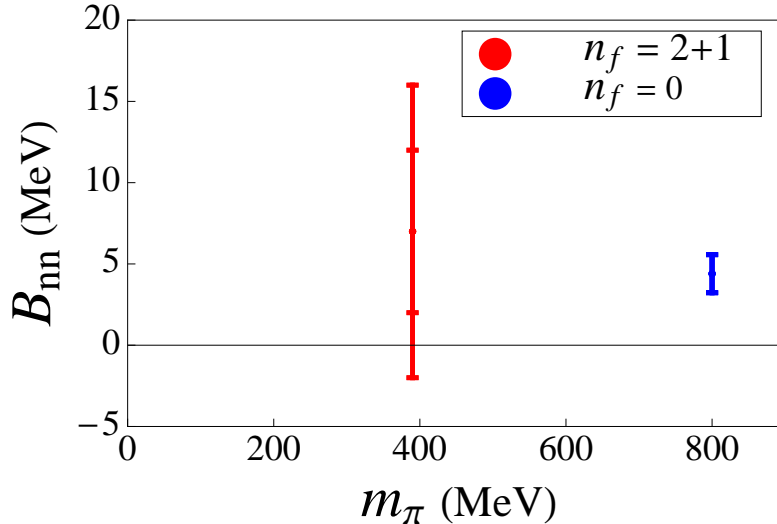


FIG. 9: The di-neutron binding energy as a function of the pion mass. The blue point and uncertainty results from the quenched calculation of Ref. [12], while the red point and uncertainty (the inner is statistical and the outer is statistical and systematic combined in quadrature) is our present $n_f = 2 + 1$ result.

C. The H-Dibaryon

The prediction of a relatively deeply bound system with the quantum numbers of $\Lambda\Lambda$ (called the H-dibaryon) by Jaffe [1] in the late 1970s, based upon a bag-model calculation, started a vigorous search for such a system, both experimentally and also with alternate theoretical tools. As all six quarks, $uuddss$, can be in an s-wave and satisfy the Pauli principle, such a channel may support a state that is more deeply bound than in channels with different flavor quantum numbers. Reviews of experimental constraints on, and phenomenological models of, the H-dibaryon can be found in Refs. [53, 54, 55, 56]. While experimental studies of doubly-strange ($s = -2$) hypernuclei restrict the H-dibaryon to be unbound or to have a small binding energy, the most recent constraints on the existence of the H-dibaryon come from heavy-ion collisions at RHIC [57], effectively eliminating the possibility of a loosely-bound H-dibaryon at the physical light-quark masses. However, the analysis that led to these constraints was model-dependent, in particular in the production mechanism, and may simply not be reliable. Recent experiments at KEK indicate that a near threshold resonance may exist in this channel [58].

A number of quenched LQCD calculations [59, 60, 61, 62, 63, 64] have previously searched for the H-dibaryon, but without success. Recently, we and the HALQCD collaboration have reported results that show that the H-dibaryon is bound for a range of light-quark masses that are larger than those found in nature [16, 17]. At present, neither of these calculations are extrapolated to the continuum, with both calculations being performed at a spatial lattice spacing of $b_s \sim 0.12$ fm. Chiral extrapolations in the light-quark masses of these two LQCD calculations were performed in Refs. [18, 19] to make first QCD predictions for the binding energy of the H-dibaryon at the physical light-quark masses.⁶

⁶ These extrapolations are significantly less reliable (rigorous) than the chiral extrapolation of simple

In the absence of interactions, the $\Lambda\Lambda$ - ΞN - $\Sigma\Sigma$ coupled system (all three have the same quantum numbers) is expected to exhibit three low-lying eigenstates as the mass-splittings between the single-particle states are (from the $32^3 \times 256$ ensemble)

$$\begin{aligned} 2(M_\Sigma - M_\Lambda) &= 0.01317(13)(19) \text{ t.l.u.} , \\ M_\Xi + M_N - 2M_\Lambda &= 0.003397(61)(65) \text{ t.l.u.} . \end{aligned} \quad (19)$$

However, if the interaction generates a bound state, it is unlikely that a second or third state will also be bound, and therefore the splitting between the ground state and the two additional states will likely be larger than estimates based upon the single-baryon masses. The EMPs associated with the Λ and the system with the quantum numbers of the $\Lambda\Lambda$ are shown in the left panels of fig. 10 and fig. 11. The binding energies extracted from the

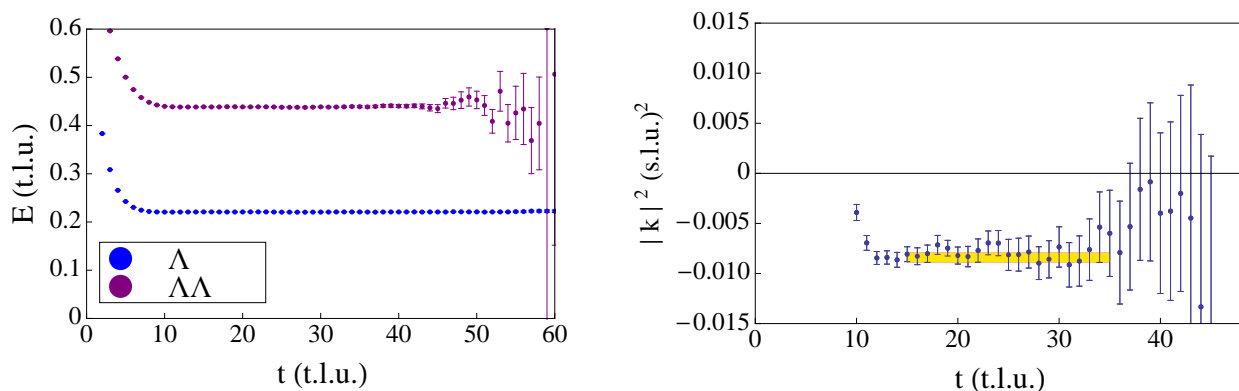


FIG. 10: The left panel shows an EMP of the Λ and of the lowest state in the $\Lambda\Lambda$ - ΞN - $\Sigma\Sigma$ system calculated with the $24^3 \times 128$ ensemble (in t.l.u.). The right panel shows the $|\mathbf{k}|^2$ (in (s.l.u.)²) of the $\Lambda\Lambda$ - ΞN - $\Sigma\Sigma$ system calculated with this ensemble, along with the fits.

quantities (such as hadron masses) calculated with LQCD. While for a deeply bound H-dibaryon with a radius that is much smaller than the inverse pion mass it is possible to arrive at a chiral EFT construction with which to calculate the light-quark mass dependence of H-dibaryon mass in perturbation theory, the same construction would not be valid when the radius becomes comparable to or larger than $1/m_\pi$. A weakly bound state can only be generated nonperturbatively, and consequently the quark-mass dependence of the binding energy is nontrivial, as is clear from the analyses in the two-nucleon sector, e.g. Refs. [45, 46, 47, 65]. As a result, the assumption of compactness of the state made in Ref. [19] is difficult to justify over a significant range of predicted binding energies. Further, the simple polynomial extrapolations in Ref. [18] are meant to provide estimates alone and cannot be used to reliably quantify extrapolation uncertainties.

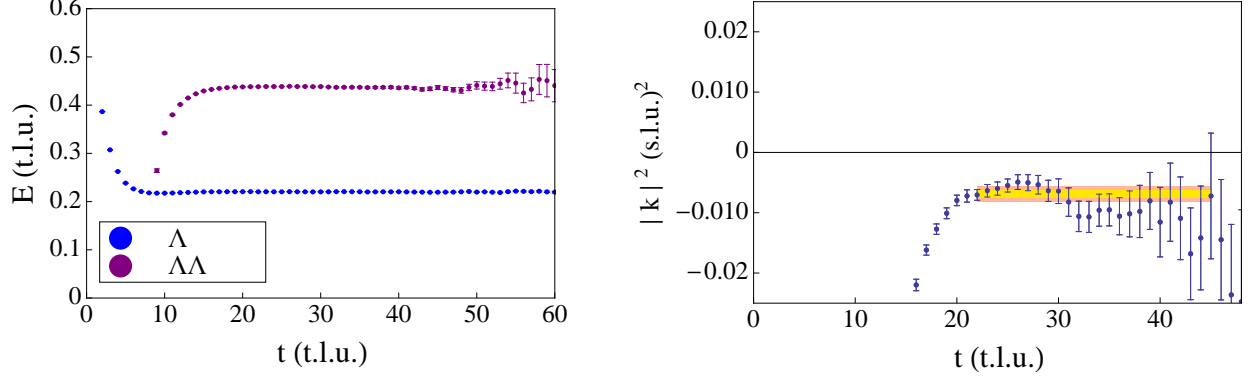


FIG. 11: The left panel shows an EMP of the Λ and of the lowest state in the $\Lambda\Lambda$ - ΞN - $\Sigma\Sigma$ system calculated with the $32^3 \times 256$ ensemble (in t.l.u.). The right panel shows the $|\mathbf{k}|^2$ (in (s.l.u.)²) of the $\Lambda\Lambda$ - ΞN - $\Sigma\Sigma$ system calculated with this ensemble, along with the fits.

LQCD calculations are

$$B_H^{(L=24)} = 17.52 \pm 0.88 \pm 0.68 \text{ MeV} \quad , \quad B_H^{(L=32)} = 14.5 \pm 1.3 \pm 2.4 \text{ MeV} \quad , \quad (20)$$

which agree within uncertainties with the values given in our earlier paper [16]. The volume extrapolation of the results in eq. (20) is shown in fig. 12, and gives an extrapolated H-dibaryon binding energy of

$$B_H^{(L=\infty)} = 13.2 \pm 1.8 \pm 4.0 \text{ MeV} \quad (21)$$

where the first uncertainty is statistical and the second is systematic. In Ref. [16], $B_H^{(L=\infty)}$

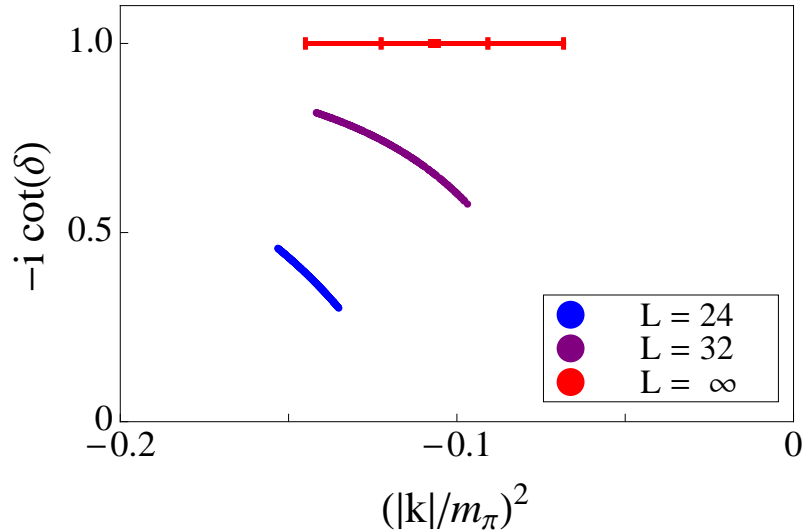


FIG. 12: The results of the LQCD calculations of $-i \cot \delta$ versus $|\mathbf{k}|^2/m_\pi^2$ in the H-dibaryon channel obtained using eq. (7), along with the infinite-volume extrapolation using eq. (10). The statistical and systematic uncertainties have been combined in quadrature.

was assigned a volume extrapolation uncertainty of ± 1 MeV. In the present analysis, this

systematic uncertainty has been reduced to ± 0.3 MeV by working to higher orders in the volume expansion [28]. The uncertainty in the energy-momentum relation is unchanged, and is estimated to be ± 0.6 MeV. The updated result in eq. (21) at $m_\pi \sim 390$ MeV and the result of the $n_f = 3$ calculation at $m_\pi \sim 837$ MeV [17] are shown in fig. 13. Also shown in this figure are two naive extrapolations, one that is linear in m_π and one that is quadratic in m_π , as discussed in Ref. [18]. The extrapolations indicate that the LQCD calculations

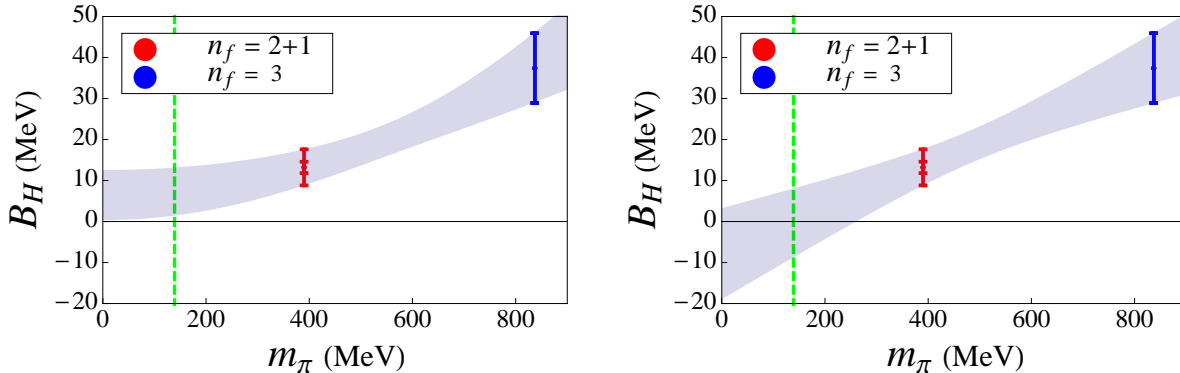


FIG. 13: Extrapolations of the LQCD results for the binding of the H-dibaryon. The left panel corresponds to an extrapolation that is quadratic in m_π , of the form $B_H(m_\pi) = B_0 + d_1 m_\pi^2$. The right panel is the same as a left panel except with an extrapolation of the form $B_H(m_\pi) = \tilde{B}_0 + \tilde{d}_1 m_\pi$. In each panel, The blue point and uncertainty results from the $n_f = 3$ LQCD calculation of Ref. [17], while the red point and uncertainty is our present $n_f = 2 + 1$ result. The green dashed vertical line corresponds to the physical pion mass.

are presently not at sufficiently small quark masses to determine if the H-dibaryon is bound at the physical light-quark masses.

D. $\Xi^- \Xi^-$

Experimental information on the hyperon-hyperon interactions in the $s < -2$ sector does not exist, presenting a significant handicap to studies of the composition of neutron star matter. As an example of the importance of these interactions, Ref. [66] shows that when a strongly attractive $\Xi \Xi$ interaction is used in the Tolman-Oppenheimer-Volkoff equation, new stable solutions appear, corresponding to compact hyperon stars with masses similar to neutron stars but with smaller radii. From the theoretical point of view, the approximate flavor SU(3) symmetry of QCD indicates that a bound state in the $\Xi^- \Xi^-$ channel is likely. Phenomenological analyses of NN scattering and YN scattering provide a determination of the strength of the interaction for two baryons in the **27** irreducible representation of flavor SU(3) that also contains the $\Xi^- \Xi^-$ system. The OBE model developed by the Nijmegen group, NSC99 [2]⁷, which include explicit breaking of flavor SU(3) symmetry by using the physical meson and baryon masses, and chiral EFT [67], predicts a bound state in the $\Xi^- \Xi^-$ channel [3, 4] at the physical pion mass⁸. However, only moderate attraction is obtained

⁷ The recently developed extended soft-core models do not yet include the $s < -2$ sectors.

⁸ The $\Xi \Xi(^3S_1)$ and $NN(^3S_1)$ states belong to different irreducible representations (**10** and $\overline{\mathbf{10}}$, respectively) and therefore SU(3) flavor symmetry alone is unable to predict whether an analog of the deuteron in the

within a constituent quark model [68]. A small $\Xi^- \Xi^-$ interaction was calculated in the $20^3 \times 128$ ensemble [8] used in this work but may be subject to significant finite volume uncertainties. LQCD calculations performed in the flavor SU(3) limit [69], in volumes of $16^3 \times 32$ with a lattice spacing of $b_s \sim 0.12$ fm and at pion masses of 1014 and 835 MeV found attractive interactions in the flavor singlet t -channel responsible for $\Xi^- \Xi^-$ interactions.

Our present LQCD calculations provide clear evidence for a bound $\Xi^- \Xi^-$ state at a pion mass of $m_\pi \sim 390$ MeV. The EMPs associated with the Ξ and the $\Xi^- \Xi^-$ system are shown in the left panels of fig. 14 and fig. 15.

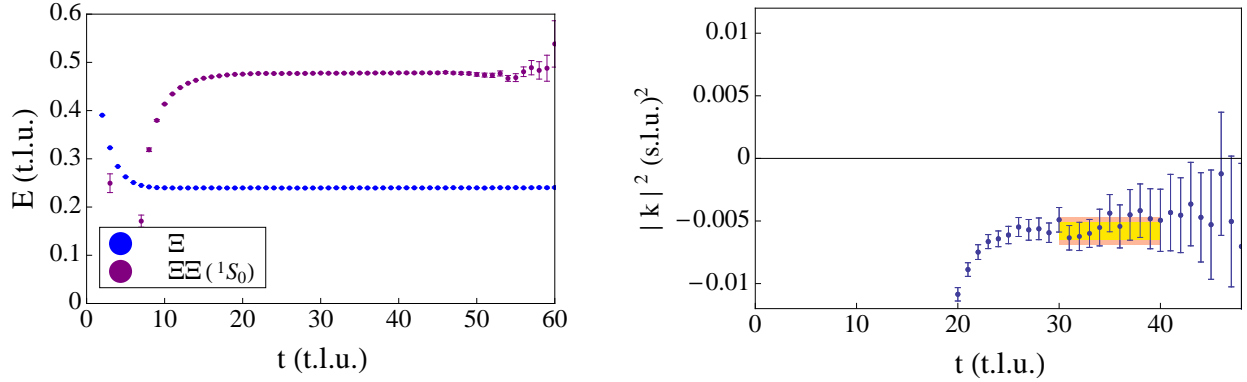


FIG. 14: The left panel shows an EMP of the Ξ and of the $\Xi^- \Xi^-$ system calculated with the $24^3 \times 128$ ensemble (in t.l.u.). The right panel shows the $|\mathbf{k}|^2$ (in (s.l.u.)²) of the $\Xi^- \Xi^-$ system calculated with this ensemble, along with the fits.

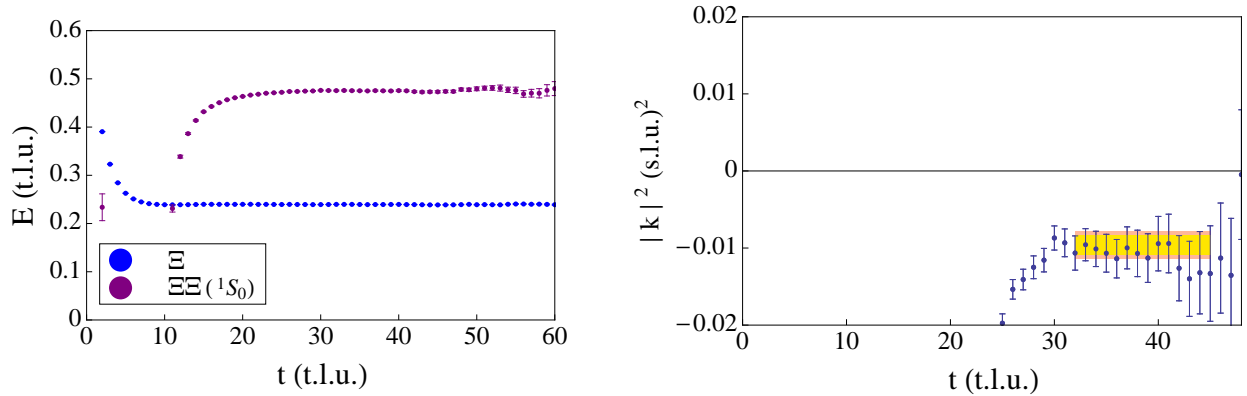


FIG. 15: The left panel shows an EMP of the Ξ and of the $\Xi^- \Xi^-$ system calculated with the $32^3 \times 256$ ensemble (in t.l.u.). The right panel shows the $|\mathbf{k}|^2$ (in (s.l.u.)²) of the $\Xi^- \Xi^-$ system calculated with this ensemble, along with the fits.

The $\Xi^- \Xi^-$ binding energies extracted from the LQCD calculations are

$$B_{\Xi^- \Xi^-}^{(L=24)} = 11.0 \pm 1.3 \pm 1.6 \text{ MeV} \quad , \quad B_{\Xi^- \Xi^-}^{(L=32)} = 13.0 \pm 0.5 \pm 3.9 \text{ MeV} \quad . \quad (22)$$

$s = -4$ sector exists.

The volume extrapolation of the results in eq. (22) is shown in fig. 16, and results in an extrapolated $\Xi^-\Xi^-$ binding energy of

$$B_{\Xi^-\Xi^-}^{(L=\infty)} = 14.0 \pm 1.4 \pm 6.7 \text{ MeV} \quad (23)$$

where the first uncertainty is statistical and the second is systematic. This indicates that, at the $\sim 2\sigma$ level, the $\Xi^-\Xi^-$ channel supports a bound state. The fact that the binding energy

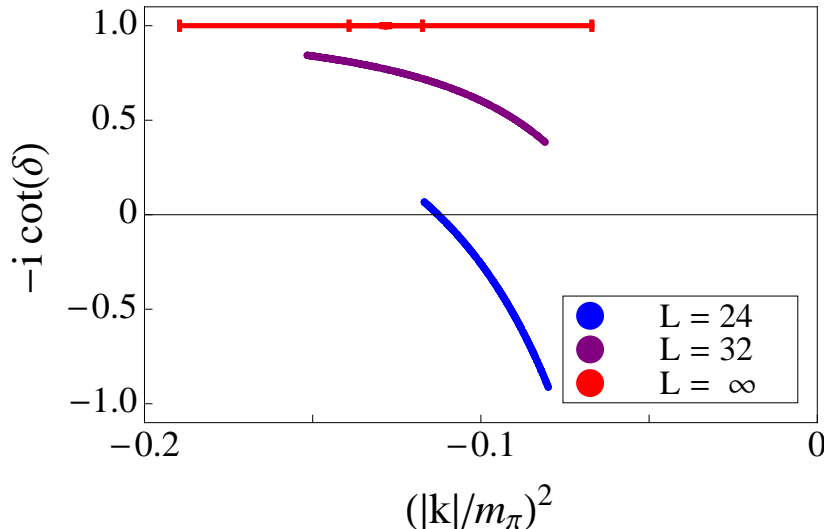


FIG. 16: The results of the Lattice QCD calculations of $-i \cot \delta$ versus $|\mathbf{k}|^2/m_\pi^2$ in the $\Xi^-\Xi^-$ system obtained using eq. (7), along with the infinite-volume extrapolation using eq. (10). The inner uncertainty of the infinite-volume extrapolation is statistical, while the outer corresponds to the statistical and systematic uncertainties combined in quadrature.

calculated in the $24^3 \times 128$ ensemble has $k \cot \delta \gtrsim 0$ indicates that this volume is significantly modifying the $\Xi^-\Xi^-$ bound state, and that calculations in larger volumes, or with non-zero total momentum, would refine the volume extrapolation.

This result and the predictions of OBE models and leading order (LO) EFT are shown in fig. 17. It is important to note that the uncertainty (and significance) of the LQCD result is comparable to that of the OBE models and EFT results. Further, this result demonstrates that LQCD is rapidly approaching the situation where it will provide more precise constraints on exotic systems than can be achieved in the laboratory. It will be interesting to see whether J-PARC [70] or FAIR [71] can provide constraints on the $s = -3$ and $s = -4$ systems, as well as on the possible H-dibaryon [72]. The binding energy in eq. (23) provides strong motivation to return to OBE models and EFT frameworks and determine the expected dependence on the light-quark masses.

E. $\Sigma^-\Sigma^-$

As the $\Sigma^-\Sigma^-$ (1S_0) system is in the **27** irreducible representation of flavor SU(3), it is also expected to be bound, but by somewhat less than the $\Xi^-\Xi^-$ system. While the NSC97a-NSC97f models [2] estimate the $\Sigma^-\Sigma^-$ binding, $B_{\Sigma^-\Sigma^-}$, to lie in the range $1.5 \text{ MeV} \lesssim B_{\Sigma^-\Sigma^-} \lesssim 3.2 \text{ MeV}$, large and negative scattering lengths are found in the $\Sigma^-\Sigma^-$

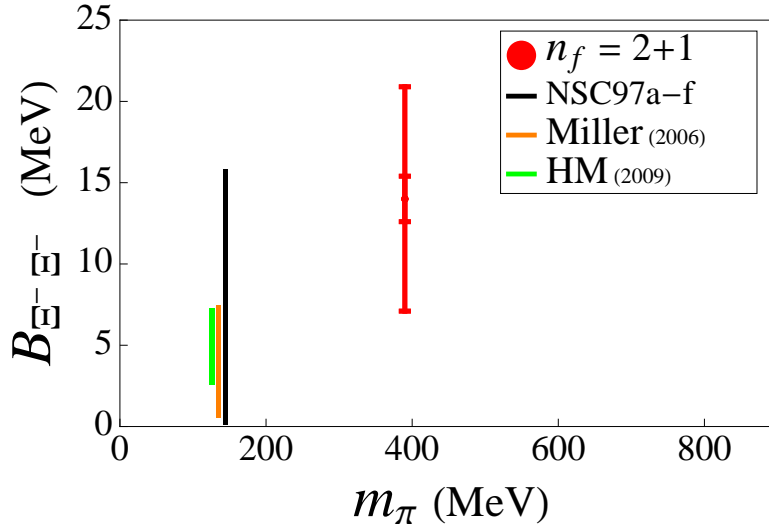


FIG. 17: The $\Xi^- \Xi^-$ binding energy as a function of the pion mass. The black line denotes the predictions of the NSC97a-NSC97f models [2] constrained from nucleon-nucleon and hyperon-nucleon scattering data. The orange line denotes the range of predictions by Miller [3], and the green line denotes the leading order EFT prediction by Haidenbauer and Meißner (HM) [4]. The red point and uncertainty (the inner is statistical and the outer is statistical and systematic combined in quadrature) is our present $n_f = 2 + 1$ result. The OBE model and EFT predictions at the physical pion mass are displaced horizontally for the purpose of display.

channel with LO EFT [73] in the absence of Coulomb interactions and isospin breaking (these results exhibit non-negligible dependence on the momentum cut-off). On the other hand, the constituent quark model of Ref. [68] finds strong similarities between the behavior of the $\Sigma^- \Sigma^-$ and nn interactions, leading to similar values for the phase shifts. Our LQCD calculations in this channel are inconclusive. While the ground state in the $24^3 \times 128$ ensemble is negatively shifted, the ground state in the $32^3 \times 256$ ensemble is consistent with zero, and thus is consistent with both a scattering state and a bound state.

V. CONCLUSIONS

We have performed precise Lattice QCD calculations of baryon-baryon systems at a pion mass of $m_{\pi} \sim 390$ MeV in four ensembles of anisotropic Clover gauge-field configurations with a spatial lattice spacing of $b_s \sim 0.123$ fm, an anisotropy of $\xi \sim 3.5$ and cubic spatial lattice volumes with extent $L \sim 2.0, 2.5, 3.0$ and 4.0 fm. These calculations have provided evidence, with varying levels of significance, for the existence of two-baryon bound states from QCD, which are summarized in Table III. Our LQCD calculations were performed

TABLE III: A summary of the two-body binding energies determined in this work.

	Deuteron	Di-neutron	H-dibaryon	$\Xi^- \Xi^-$
Binding Energy (MeV)	11(05)(12)	7.1(5.2)(7.3)	13.2(1.8)(4.0)	14.0(1.4)(6.7)

at one lattice spacing, $b_s \sim 0.123$ fm, but discretization effects are expected to be small as they scale as $\mathcal{O}(b_s^2)$ for the Clover action. Consequently, we do not expect them to significantly alter our conclusions. A second lattice spacing is required to quantify this systematic uncertainty.

By far the most significant result is that the H-dibaryon is bound at the 3σ level at this pion mass, improving on results we have already presented in Ref. [16]. At the $\sim 2\sigma$ level of significance, we find that the $\Xi^-\Xi^-$ system is also bound, which is qualitatively consistent with an array of hadronic models and EFT analyses of this system at the physical light-quark masses. It is interesting to note that the level of precision of the $\Xi^-\Xi^-$ binding from LQCD is comparable to the level of precision associated with the phenomenological predictions. With increasing computational resources directed at these two-baryon systems, the QCD prediction will become more precise and eventually become input for phenomenological models and will be used to constrain the coefficients appearing in the effective field theories.

A major goal of Lattice QCD is to postdict the anomalously small binding energy of the deuteron. We have presented evidence for a bound deuteron from QCD, however the $\sim 1\sigma$ level of significance is well below “discovery level”, and our result should be considered a first step toward a definitive calculation. Nevertheless, it is now unambiguously clear that a precise determination of the deuteron binding energy can be performed with sufficient computational resources. Our result hints that the deuteron is bound, as does the result of a previous quenched calculation, at heavy pion masses, in contrast with phenomenological analyses and with EFT predictions. We also find suggestions of a bound di-neutron which are far from definitive, but are consistent with the quenched result at a heavier pion mass [12]. If this remains the case when the calculation is refined, there are light-quark masses between $m_\pi \sim 140$ MeV and $m_\pi \sim 390$ MeV for which the scattering length in this channel would be infinite and the system would be scale-invariant at low energies.

Phenomenology based upon flavor SU(3) symmetry indicates that the $\Xi^-\Xi^-$ system should be more bound than the $\Sigma^-\Sigma^-$ system, which in turn should be more bound than the di-neutron (which is nearly bound) at the physical light-quark masses, as these three systems are all members of the same **27** irreducible representation of SU(3). Our results are consistent with this, but further work is required before definitive conclusions can be drawn.

The results of the Lattice QCD calculations presented in this paper, which refine and broaden our previous work [16], provide clear evidence for bound-states of two baryons directly from QCD. With the suggestion of a deuteron and a bound di-neutron at this heavier pion mass, there is compelling motivation to invest larger computational resources into pursuing Lattice QCD calculations at light-quark masses, and to perform such calculations in multiple volumes and with multiple lattice spacings. It is clear that enhanced computational resources will enable calculations of the properties and interactions of nuclei from QCD with quantifiable and systematically removable uncertainties.

We would like to thank G. A. Miller for interesting discussions. We thank K. Roche for computing resources at ORNL NCCS, and B. Joó for a significant contribution to our running. We thank R. Edwards and B. Joó for help with QDP++ and Chroma [74]. We acknowledge computational support from the USQCD SciDAC project, the National Energy Research Scientific Computing Center (NERSC, Office of Science of the US DOE, DE-AC02-05CH11231), the UW HYAK facility, Centro Nacional de Supercomputación (Barcelona, Spain), LLNL, and the NSF through Teragrid resources provided by TACC and NICS under grant number TG-MCA06N025. SRB was supported in part by the NSF CAREER grant PHY-0645570.

The work of EC and AP is supported by the contract FIS2008-01661 from MEC (Spain) and FEDER. AP acknowledges support from the RTN Flavianet MRTN-CT-2006-035482 (EU). H-WL and MJS were supported in part by the DOE grant DE-FG03-97ER4014. WD and KO were supported in part by DOE grants DE-AC05-06OR23177 (JSA) and DE-FG02-04ER41302. WD was also supported by DOE OJI grant de-sc0001784 and Jeffress Memorial Trust, grant J-968. KO was also supported in part by NSF grant CCF-0728915 and DOE OJI grant DE-FG02-07ER41527. AT was supported by NSF grant PHY-0555234 and DOE grant DE-FC02-06ER41443. The work of TL was performed under the auspices of the U.S. Department of Energy by LLNL under Contract DE-AC52-07NA27344. The work of AWL was supported in part by the Director, Office of Energy Research, Office of High Energy and Nuclear Physics, Divisions of Nuclear Physics, of the U.S. DOE under Contract No. DE-AC02-05CH11231

-
- [1] R. L. Jaffe, Phys. Rev. Lett. **38**, 195 (1977); **38**, 617 (1977)(E).
 - [2] V. G. J. Stoks and T. A. Rijken, Phys. Rev. C **59**, 3009 (1999) [arXiv:nucl-th/9901028].
 - [3] G. A. Miller, arXiv:nucl-th/0607006.
 - [4] J. Haidenbauer, U. -G. Meißner, Phys. Lett. **B684**, 275-280 (2010). [arXiv:0907.1395 [nucl-th]].
 - [5] M. Fukugita, Y. Kuramashi, H. Mino, M. Okawa and A. Ukawa, Phys. Rev. Lett. **73**, 2176 (1994) [arXiv:hep-lat/9407012].
 - [6] M. Fukugita, Y. Kuramashi, M. Okawa, H. Mino and A. Ukawa, Phys. Rev. D **52**, 3003 (1995) [arXiv:hep-lat/9501024].
 - [7] S. R. Beane, P. F. Bedaque, K. Orginos and M. J. Savage, Phys. Rev. Lett. **97**, 012001 (2006) [arXiv:hep-lat/0602010].
 - [8] S. R. Beane *et al.* [NPLQCD Collaboration], Phys. Rev. D **81**, 054505 (2010) [arXiv:0912.4243 [hep-lat]].
 - [9] S. Aoki, T. Hatsuda and N. Ishii, Comput. Sci. Dis. **1**, 015009 (2008) [arXiv:0805.2462 [hep-ph]].
 - [10] S. Aoki, T. Hatsuda and N. Ishii, Prog. Theor. Phys. **123**, 89 (2010) [arXiv:0909.5585 [hep-lat]].
 - [11] N. Ishii, S. Aoki and T. Hatsuda, Phys. Rev. Lett. **99**, 022001 (2007) [arXiv:nucl-th/0611096].
 - [12] T. Yamazaki, Y. Kuramashi, A. Ukawa, arXiv:1105.1418 [hep-lat].
 - [13] T. Yamazaki, Y. Kuramashi, A. Ukawa, Phys. Rev. D **81**, 111504 (2010) [arXiv:0912.1383 [hep-lat]].
 - [14] S. R. Beane *et al.*, Phys. Rev. D **80**, 074501 (2009) [arXiv:0905.0466 [hep-lat]].
 - [15] P. de Forcrand and M. Fromm, Phys. Rev. Lett. **104**, 112005 (2010) [arXiv:0907.1915 [hep-lat]].
 - [16] S. R. Beane *et al.* [NPLQCD Collaboration], Phys. Rev. Lett. **106**, 162001 (2011) [arXiv:1012.3812 [hep-lat]].
 - [17] T. Inoue *et al.* [HAL QCD Collaboration], Phys. Rev. Lett. **106**, 162002 (2011) [arXiv:1012.5928 [hep-lat]].
 - [18] S. R. Beane *et al.*, arXiv:1103.2821 [hep-lat].
 - [19] P. E. Shanahan, A. W. Thomas and R. D. Young, arXiv:1106.2851 [nucl-th].
 - [20] S. R. Beane *et al.*, Phys. Rev. D **79**, 114502 (2009) [arXiv:0903.2990 [hep-lat]].
 - [21] S. R. Beane *et al.*, Phys. Rev. D **84**, 014507 (2011) [arXiv:1104.4101 [hep-lat]].

- [22] H. W. Hamber, E. Marinari, G. Parisi and C. Rebbi, Nucl. Phys. B **225**, 475 (1983).
- [23] M. Lüscher, Commun. Math. Phys. **105**, 153 (1986).
- [24] M. Lüscher, Nucl. Phys. B **354**, 531 (1991).
- [25] M. Lüscher, Commun. Math. Phys. **104**, 177 (1986).
- [26] S. R. Beane, P. F. Bedaque, A. Parreno and M. J. Savage, Phys. Lett. B **585**, 106 (2004) [arXiv:hep-lat/0312004].
- [27] S. Bour, S. Konig, D. Lee, H. W. Hammer and U. G. Meißner, arXiv:1107.1272 [nucl-th].
- [28] Z. Davoudi and M. J. Savage, arXiv:1108.5371 [hep-lat].
- [29] M. Okamoto *et al.* [CP-PACS Collaboration], Phys. Rev. D **65**, 094508 (2002) [arXiv:hep-lat/0112020].
- [30] P. Chen, Phys. Rev. D **64**, 034509 (2001) [arXiv:hep-lat/0006019].
- [31] C. Morningstar and M. J. Peardon, Phys. Rev. D **69**, 054501 (2004) [arXiv:hep-lat/0311018].
- [32] H. W. Lin *et al.* [Hadron Spectrum Collaboration], Phys. Rev. D **79**, 034502 (2009) [arXiv:0810.3588 [hep-lat]].
- [33] R. G. Edwards, B. Joó and H. W. Lin, Phys. Rev. D **78**, 054501 (2008) [arXiv:0803.3960 [hep-lat]].
- [34] J. J. Dudek, R. G. Edwards, M. J. Peardon, D. G. Richards and C. E. Thomas, Phys. Rev. Lett. **103**, 262001 (2009) [arXiv:0909.0200 [hep-ph]].
- [35] J. Bulava *et al.*, Phys. Rev. D **82** (2010) 014507 [arXiv:1004.5072 [hep-lat]].
- [36] J. J. Dudek, R. G. Edwards, B. Joo, M. J. Peardon, D. G. Richards, C. E. Thomas, Phys. Rev. D **83**, 111502 (2011). [arXiv:1102.4299 [hep-lat]].
- [37] C. Morningstar, J. Bulava, J. Foley, K. J. Juge, D. Lenkner, M. Peardon and C. H. Wong, Phys. Rev. D **83**, 114505 (2011) [arXiv:1104.3870 [hep-lat]].
- [38] R. G. Edwards, J. J. Dudek, D. G. Richards, S. J. Wallace, [arXiv:1104.5152 [hep-ph]].
- [39] H. -W. Lin, S. D. Cohen, [arXiv:1108.2528 [hep-lat]].
- [40] S. R. Beane, W. Detmold, K. Orginos, M. J. Savage, Prog. Part. Nucl. Phys. **66**, 1, (2011) [arXiv:1004.2935 [hep-lat]].
- [41] P. F. Bedaque, I. Sato and A. Walker-Loud, Phys. Rev. D **73**, 074501 (2006) [arXiv:hep-lat/0601033].
- [42] I. Sato and P. F. Bedaque, Phys. Rev. D **76**, 034502 (2007) [arXiv:hep-lat/0702021].
- [43] C. Aubin, K. Orginos, [arXiv:1010.0202 [hep-lat]].
- [44] K. Orginos PoS(Lattice 2010)118
- [45] S. R. Beane and M. J. Savage, Nucl. Phys. A **713**, 148 (2003) [arXiv:hep-ph/0206113].
- [46] E. Epelbaum, U. G. Meißner and W. Gloeckle, Nucl. Phys. A **714**, 535 (2003) [arXiv:nucl-th/0207089].
- [47] S. R. Beane and M. J. Savage, Nucl. Phys. A **717**, 91 (2003) [arXiv:nucl-th/0208021].
- [48] J. W. Chen, T. K. Lee, C. P. Liu and Y. S. Liu, arXiv:1012.0453 [nucl-th].
- [49] V. V. Flambaum and R. B. Wiringa, Phys. Rev. C **76**, 054002 (2007) [arXiv:0709.0077 [nucl-th]].
- [50] P. F. Bedaque, T. Luu, L. Platter, Phys. Rev. C **83**, 045803 (2011). [arXiv:1012.3840 [nucl-th]].
- [51] M. K. Cheoun, T. Kajino, M. Kusakabe and G. J. Mathews, arXiv:1104.5547 [astro-ph.CO].
- [52] E. Braaten, H. W. Hammer, Phys. Rev. Lett. **91**, 102002 (2003). [nucl-th/0303038].
- [53] S. Bashinsky and R. L. Jaffe, Nucl. Phys. A **625**, 167 (1997) [arXiv:hep-ph/9705407].
- [54] K. Yamamoto *et al.*, Phys. Lett. B **478** (2000) 401.
- [55] T. Sakai, K. Shimizu and K. Yazaki, Prog. Theor. Phys. Suppl. **137**, 121 (2000) [arXiv:nucl-th/9912063].

- [56] P. J. Mulders and A. W. Thomas, *J. Phys. G* **9**, 1159 (1983).
- [57] A. L. Trattner, PhD Thesis, LBL, UMI-32-54109 (2006).
- [58] C. J. Yoon *et al.*, *Phys. Rev. C* **75**, 022201 (2007).
- [59] P. B. Mackenzie and H. B. Thacker, *Phys. Rev. Lett.* **55**, 2539 (1985).
- [60] Y. Iwasaki, T. Yoshie and Y. Tsuboi, *Phys. Rev. Lett.* **60**, 1371 (1988).
- [61] A. Pochinsky, J. W. Negele and B. Scarlet, *Nucl. Phys. Proc. Suppl.* **73**, 255 (1999) [arXiv:hep-lat/9809077].
- [62] I. Wetzorke, F. Karsch and E. Laermann, *Nucl. Phys. Proc. Suppl.* **83**, 218 (2000) [arXiv:hep-lat/9909037].
- [63] I. Wetzorke and F. Karsch, *Nucl. Phys. Proc. Suppl.* **119**, 278 (2003) [arXiv:hep-lat/0208029].
- [64] Z. H. Luo, M. Loan and X. Q. Luo, *Mod. Phys. Lett. A* **22**, 591 (2007) [arXiv:0803.3171 [hep-lat]].
- [65] J. Mondejar, J. Soto, *Eur. Phys. J.* **A32**, 77-85 (2007). [nucl-th/0612051].
- [66] J. Schaffner-Bielich, M. Hanauske, H. Stoecker and W. Greiner, arXiv:astro-ph/0005490.
- [67] M. J. Savage and M. B. Wise, *Phys. Rev. D* **53**, 349 (1996) [arXiv:hep-ph/9507288].
- [68] Y. Fujiwara, Y. Suzuki and C. Nakamoto, *Prog. Part. Nucl. Phys.* **58**, 439 (2007) [arXiv:nucl-th/0607013].
- [69] T. Inoue *et al.* [HAL QCD collaboration], *Prog. Theor. Phys.* **124**, 591 (2010) [arXiv:1007.3559 [hep-lat]].
- [70] http://j-parc.jp/NuclPart/index_e.html
- [71] J. Steinheimer, M. Mitrovski, T. Schuster, H. Petersen, M. Bleicher and H. Stoecker, *Phys. Lett. B* **676**, 126 (2009) [arXiv:0811.4077 [hep-ph]].
- [72] http://j-parc.jp/NuclPart/pac_1107/pdf/KEK_J-PARC-PAC2011-03.pdf
- [73] H. Polinder, J. Haidenbauer and U. G. Meißner, *Phys. Lett. B* **653**, 29 (2007) [arXiv:0705.3753 [nucl-th]].
- [74] R. G. Edwards and B. Joó, *Nucl. Phys. Proc. Suppl.* **140** (2005) 832.